The Astronomical Journal, 128:2593–2598, 2004 November

ASTROMETRY OF 25 SOUTHERN HEMISPHERE RADIO SOURCES FROM A VLBI SHORT-BASELINE SURVEY

Alan L. Fey
US Naval Observatory, 3450 Massachusetts Avenue, NW, Washington, DC 20392-5420

Roopesh Ojha and John E. Reynolds
Australia Telescope National Facility, CSIRO, P.O. Box 76, Epping, NSW 1710, Australia

Simon P. Ellingsen and Peter M. McCulloch
School of Mathematics and Physics, Private Bag 37, University of Tasmania, Hobart, Tasmania 7001, Australia

David L. Jauncey
Australia Telescope National Facility, CSIRO, P.O. Box 76, Epping, NSW 1710, Australia

and

Kenneth J. Johnston
US Naval Observatory, 3450 Massachusetts Avenue, NW, Washington, DC 20392-5420
Received 2004 July 2; accepted 2004 August 5

ABSTRACT

Milliarcsecond-accurate radio positions for 25 southern hemisphere extragalactic sources are reported. These positions are derived from Mark III Very Long Baseline Interferometry observations made between 2003 September and 2004 May on the intra-Australia baseline connecting Hobart, Tasmania and Parkes, New South Wales. The results presented here represent an ongoing program intended to increase the number of phase-reference sources with accurate positions in the southern hemisphere for use in astrophysical observations. The positions for all but 1 of the 25 sources are south of $\delta = -45°$ and have average formal uncertainties of 3 mas in $\alpha \cos \delta$ and 2 mas in δ. As the reported positions are in the frame of the International Celestial Reference Frame (ICRF), the results reported here can also be used to increase the sky density of southern hemisphere ICRF sources, although with reduced accuracy.

Key words: astrometry — catalogs — quasars: general — radio continuum: galaxies — reference systems — techniques: interferometric

1. INTRODUCTION

The Australia Telescope National Facility (ATNF) and the United States Naval Observatory (USNO) are currently leading a collaboration in a continuing very long baseline interferometry (VLBI) research program in southern hemisphere astrometry and source imaging. The primary goals of this program are to increase the sky density of International Celestial Reference Frame (ICRF; Ma et al. 1998; Fey et al. 2004a) sources in the southern hemisphere and to image their milliarcsecond-scale structure for monitoring. Milliarcsecond-accurate radio positions for 22 new southern hemisphere extragalactic sources have been recently reported by Fey et al. (2004b), and initial results of the imaging program have been reported by Ojha et al. (2004).

Our early southern hemisphere VLBI astrometry programs (Russell et al. 1992, 1994; Reynolds et al. 1994; Johnston et al. 1995) provided the fundamental basis for the ICRF in the southern hemisphere, as well as the basis for the southern component of the Australia Telescope Compact Array (ATCA) position calibrator list currently in use. However, since these early programs over a decade ago, there has been only marginal improvement to the ATCA calibrator list. In order to provide additional calibrators for phase-referencing use, we have initiated a program of southern hemisphere astrometry, in conjunction with our ICRF astrometry program, with the specific intent of obtaining accurate positions for new southern hemisphere sources not currently in the ATCA calibrator list or in the ICRF.

In this paper, we use astrometric VLBI observations obtained between 2003 September and 2004 May to estimate milliarcsecond-accurate radio positions for 25 southern hemisphere radio sources. These observations provide improved positions for six existing ATCA calibrators, as well as accurate positions for 19 new sources, thus increasing the sky density of the ATCA calibrator list and thereby improving the science potential of this instrument. All but one of the observed sources are south of $\delta = -45°$, where the need to increase the density of ATCA calibrators is particularly acute. Furthermore, these astrometric observations provide more sources with sufficiently accurate positions in order to conduct phase-referenced VLBI observations with the Australian Long Baseline Array (LBA). Note, for example, that many of the present Very Long Baseline Array observations are undertaken in phase-referencing mode, something that is seldom possible with the LBA because of the lack of a dense grid of phase calibration sources. Additionally, as the reported positions are in the frame of the ICRF, the results reported here can also be used to increase the sky density of southern hemisphere ICRF sources, although with reduced accuracy.

2. OBSERVATIONS

In order to identify new compact radio sources to be used as ATCA and LBA phase-reference calibrators, survey observations of selected flat-spectrum extragalactic sources from Lovell (1997) have been interspersed among our VLBI imaging observations (see Ojha et al. 2004 for a description of our

VLBI imaging program). The survey observations were made at a frequency of 8.4 GHz and used the S2 VLBI recording system (Cannon et al. 1997). Candidate sources for the current program were selected on the basis of positive detection on intra-Australia baselines but no detection on transoceanic baselines (i.e., baselines either between Australia and South Africa or between Australia and Hawaii). Astrometric observations of sources detected in the survey on the transoceanic baselines are the subject of future work.

These survey observations identified a total of 29 possible short-baseline astrometric targets. Because these sources were detected only on intra-Australia baselines in our survey, dedicated astrometric VLBI experiments using the intra-Australia baseline connecting Hobart, Tasmania and Parkes, New South Wales were subsequently scheduled to determine accurate positions for these sources. One additional source (PKS 1245−454) was observed to fulfill a request to obtain an improved position for an unrelated phase-referencing experiment, bringing the total number of sources observed to 30.

VLBI observations for geodesy and astrometry using Mark III compatible systems (Clark et al. 1985) have been conducted since about mid-1979. These observations are made in a bandwidth-synthesis mode at standard frequencies of 2.3 and 8.4 GHz. The bandwidths over which the group delay is synthesized are typically 85 and 360 MHz, respectively. Dual-frequency observations allow for an accurate calibration of the frequency-dependent propagation delay introduced by the ionosphere, whereas the multiplicity of channels facilitates the determination of a precise group delay (Rogers 1970). Observing sessions are typically of 24 hr duration in order to recover and separate parameters for nutation and polar motion.

Dedicated astrometric Mark III VLBI observations were scheduled on 2003 September 4, October 9, 2004 January 13, and May 12 using a VLBI array consisting of the 64 m antenna at Parkes,[1] New South Wales, Australia and the 26 m antenna at Hobart, Tasmania, Australia. All observations were correlated at the Washington Correlator (Kingham 2003). Additional astrometric observations for three of the 30 sources (PKS 1143−696, PKS 1156−663, and PKS 1420−679) were also obtained from observations on 2003 August 20 using a VLBI array consisting of the 26 m antenna at Hartebeesthoek, South Africa and the 70 m Deep Space Network antenna at Tidbinbilla, Australia Capital Territory, Australia (see Fey et al. 2004b for a description of these observations).

In addition to the 30 target sources, of order 10 ICRF sources with accurate positions were also observed in each astrometric session. These "calibrator" sources are required in order to ensure continuity between the new observing sessions and previous ones so that the new observations may be successfully linked to the ICRF (see § 3).

3. ANALYSIS

3.1. *The Software*

Accurate astrometric positions were estimated at the USNO using the Goddard Space Flight Center (GSFC) analysis system (Ryan et al. 1980, 1993; Ma et al. 1986; Caprette et al. 1990), which consists of the astrometric and geodetic VLBI reduction software CALC and SOLVE. The data analysis methods using the GSFC system are covered in detail in Ma et al. (1986). A typical analysis combines data from many different observing sessions, allowing some parameters (e.g., source positions) to be estimated from a combination of many data sets. Application of the analysis methods to the ICRF are described in detail in Ma et al. (1998). Application of the analysis methods to the two ICRF extensions are described in Fey et al. (2004a).

To obtain a solution, the individual observing sessions are combined sequentially using "arc"-parameter elimination (Ma et al. 1990). All solutions give weighted least-squares estimates for parameters. Time-invariant, or "global," parameters, i.e., parameters dependent on all data sets, are carried from step to step, resulting in a single estimate derived from the combined data of all experiments in the solution. Depending on the problem at hand, these global parameters may include station positions, station velocities, source positions, source velocities (proper motions), nutation series coefficients, the precession constant, and the Love numbers for the solid Earth tides. Local, or "arc," parameters depend only on the data from an individual experiment and are estimated separately for each epoch of observation. Arc parameters include those for the station clocks and atmospheric delay, the Earth's orientation, and nutation offsets in obliquity and longitude. Station positions and source positions can also be arc parameters if the solution is to follow changes over time.

3.2. *Radio Position Estimation*

When the ICRF was defined (Ma et al. 1998), the radio positions were based on a general solution for all applicable dual-frequency 2.3 and 8.4 GHz Mark III VLBI data available through the middle of 1995, which consisted of 1.6 million pairs of group-delay– and phase-delay–rate observations. The two ICRF extension/update solutions (Fey et al. 2004a) were parameterized similarly to the ICRF solution but differed primarily in that more recent data were added to the previous data set.

The radio positions reported here are based on a general solution similar to that for the ICRF and its extensions except that all applicable dual-frequency 2.3 and 8.4 GHz Mark III VLBI data available through the end of 2004 May, including the four dedicated experiments described in § 2, were used. This data set consisted of 4,079,296 group-delay and delay-rate measurements from 3669 24 hr observing sessions. The weighting of the data followed the ICRF solution. For each session a pair of added noise values was computed for delays and delay rates on a station-by-station basis, which caused the reduced χ^2_ν (the χ^2 per degree of freedom) to be close to unity when added to the variance of the observations derived from the correlation and fringe-finding process, as well as from the calibration of the ionosphere. The postfit weighted rms residuals of the solution were 23.75 ps (79.02 fs s^{-1}) for delay (rate) with a combined reduced χ^2_ν of 0.96. There were 1473 global parameters, 1,939,315 arc parameters, 778,720 constraints, and 6,996,524 degrees of freedom.

Similar to the ICRF solution, the primary geodetic parameters, the station positions, were estimated separately for each session in the solution. In this way, any nonlinear motion of the stations (e.g., unmodeled tectonic motion, long-term antenna motion, or earthquake displacements) does not affect the integrity of the invariant source positions. Station motions within a day, from solid Earth tides and ocean loading, were derived from unadjusted a priori models (McCarthy 1996). The adjusted arc parameters included positions of sources with identified excessive apparent motion or random variation; celestial pole offsets in ecliptic longitude and obliquity to account for

[1] The Parkes telescope is part of the Australia Telescope, which is funded by the Commonwealth of Australia for operation as a National Facility managed by CSIRO.

TABLE 1
COORDINATES OF SOURCES

Source	α (J2000.0)	δ (J2000.0)	σ_α (s)	σ_δ (arcsec)	$C_{\alpha-\delta}$	Epoch of Observation (MJD) Mean	First	Last	N_{exp}	N_{obs}
0037−593[a]	00 40 07.848794	−59 03 52.76516	0.000432	0.00200	−0.483	53,019.7	52,887.6	53,138.8	4	18
0214−522[a]	02 16 03.198150	−52 00 12.47851	0.000399	0.00179	−0.496	52,992.8	52,887.6	53,138.8	3	16
0542−735	05 41 50.775308	−73 32 15.34728	0.000519	0.00145	0.041	52,980.3	52,887.6	53,138.8	3	22
0628−627	06 28 57.488064	−62 48 44.74488	0.000445	0.00133	0.122	52,963.3	52,887.6	53,138.8	3	17
0744−691	07 44 20.393900	−69 19 07.15504	0.000716	0.00184	0.398	52,983.1	52,887.6	53,138.8	3	15
0903−573	09 04 53.179089	−57 35 05.78380	0.000305	0.00130	0.367	52,970.4	52,887.6	53,138.8	3	19
1005−739	10 06 04.144393	−74 09 44.08647	0.001033	0.00257	0.265	52,972.0	52,887.6	53,138.8	3	14
1049−650	10 51 23.521430	−65 18 08.62438	0.000474	0.00197	0.199	52,961.4	52,887.6	53,138.8	3	16
1133−739	11 36 09.659055	−74 15 45.27428	0.001010	0.00241	0.107	53,016.1	52,887.6	53,138.8	3	12
1143−696[b]	11 45 53.624164	−69 54 01.79779	0.000124	0.00074	0.329	52,941.3	52,872.9	53,138.8	4	21
1156−663[b]	11 59 18.305410	−66 35 39.42731	0.000097	0.00077	0.167	52,931.0	52,872.9	53,138.8	4	21
1245−454	12 48 28.494730	−45 59 47.17693	0.000308	0.00148	−0.007	53,092.6	53,018.7	53,138.8	2	13
1303−827	13 08 38.194317	−82 59 34.79524	0.001654	0.00389	0.261	52,984.9	52,887.6	53,138.8	3	14
1343−601	13 46 49.043210	−60 24 29.35464	0.000257	0.00102	0.145	52,991.2	52,887.6	53,138.8	4	22
1417−782	14 23 43.550261	−78 29 34.90069	0.001177	0.00301	0.229	53,016.1	52,887.6	53,138.8	3	12
1420−679[b]	14 24 55.557397	−68 07 58.09452	0.000098	0.00067	0.157	52,930.1	52,872.9	53,138.8	4	19
1448−648	14 52 39.679008	−65 02 03.43240	0.000485	0.00207	0.314	52,975.1	52,887.6	53,138.8	4	15
1508−656	15 12 51.551098	−65 53 02.22328	0.000753	0.00283	0.278	52,973.0	52,887.6	53,138.8	3	13
1611−710	16 16 30.640619	−71 08 31.45443	0.000571	0.00164	0.009	53,011.9	52,887.6	53,138.8	3	15
1637−771	16 44 16.120318	−77 15 48.81271	0.000988	0.00283	0.161	53,005.0	52,887.6	53,138.8	3	11
1725−795	17 33 40.699908	−79 35 55.71960	0.000832	0.00219	0.210	53,009.0	52,887.6	53,138.8	3	13
2117−642[a]	21 21 55.022869	−64 04 30.04192	0.000920	0.00324	−0.229	53,069.6	52,887.6	53,138.8	3	9
2215−508[a]	22 18 19.025063	−50 38 41.73103	0.000383	0.00155	0.019	53,029.7	52,887.6	53,138.8	4	19
2254−367[a]	22 57 10.607977	−36 27 43.99694	0.000474	0.00273	−0.601	53,055.0	52,887.6	53,138.8	2	9
2311−477[a]	23 13 51.900260	−47 29 11.72355	0.000382	0.00176	0.281	53,041.3	52,887.6	53,138.8	3	14

NOTE.—Units of right ascension are hours, minutes, and seconds, and units of declination are degrees, arcminutes, and arcseconds.
[a] Source already in ATCA calibrator list.
[b] Estimated position includes observations from 2003 August 20 on the South Africa–Australia baseline; see Fey et al. (2004b).

errors in the standard precession/nutation models; positions of the stations; the rate of UT1 relative to a good a priori time series; 20 minute piecewise linear continuous troposphere parameters; tropospheric gradients in the east-west and north-south directions, linear in time, estimated once per hour; quadratic clock polynomials for the gross clock behavior; 60 minute piecewise linear continuous clock parameters; and necessary nuisance parameters such as clock jumps and baseline clock offsets (i.e., separate bias parameters for each VLBI baseline to accommodate small, constant, baseline-dependent instrumental and correlator errors). The same set of sources were treated as arc parameters, as in the ICRF solution, with the exception of the following ICRF-defining sources that were downgraded in the ICRF extension solutions (Fey et al. 2004a) to arc parameters because of excessive apparent motion: 0804+499, 1308+326, 1606+106, 2037+511 (3C 418), and 2145+067. One additional source (1718−649) was downgraded to arc parameter in this solution for the same reason. The remaining parameters, including source positions, were adjusted as invariant, or "global," quantities from the entire data set.

The entire database of available observations, rather than just the four dedicated experiments, were used in the solution because these data, when combined, compose the foundation on which the reference frame is built. The resulting set of over 800 source positions defines a rigid frame that requires only a rotation into the system of the International Celestial Reference System (ICRS; Arias et al. 1995). This frame alignment was achieved through a no–net-rotation constraint imposed on the positions of 206 of the 212 ICRF-defining sources using their published positions from Ma et al. (1998). If only the four dedicated experiments were used, there would be insufficient positional information to construct a rigid frame, and no frame alignment would be possible.

The solution described here also differed from that of the ICRF solution in that the troposphere was modeled using the NMF mapping function (Niell 1996), estimating the zenith troposphere effects in the form of 20 minute piecewise linear continuous functions with a constraint of 50 ps hr^{-1} on the rate of variations.

4. RESULTS

The primary result obtained from the least-squares solution is the set of invariant source positions and their formal uncertainties. Of the initial 30 sources, no successful observations (i.e., measurement of group delay and delay rate) were obtained for the sources PKS 2101−715, 2134−470, 2226−411, and 2310−417. The source PKS 0806−710 had only one successful observation. The remaining 25 sources were observed with nine or more successful observations obtained during at least two or more 24 hr observing sessions. Six of these sources are existing ATCA calibrators. The remaining sources are not currently in the ATCA calibrator list. All 25 sources are new to the ICRF.

Positions for the observed sources are listed in Table 1. The column labeled $C_{\alpha-\delta}$ lists the correlation between right ascension and declination. The column labeled N_{exp} lists the number of 24 hr observing sessions, and N_{obs} lists the number of observations. As a direct result of the no–net-rotation

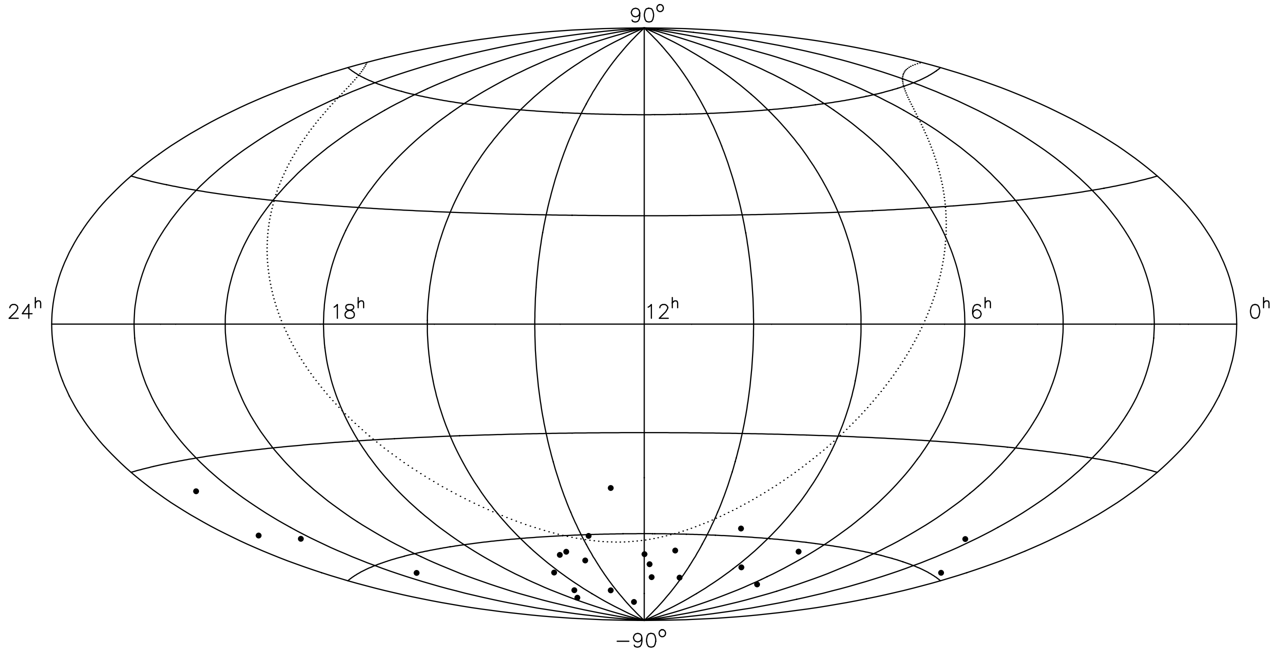

Fig. 1.—Distribution of sources on an Aitoff equal-area projection of the celestial sphere. The dotted line represents the Galactic equator.

constraint described in § 3.2, the positions listed in Table 1 are given directly in the frame of the ICRF.

The distribution on the sky of the new sources is shown in Figure 1. Note that the positions for all but 1 of the 25 sources are south of $\delta = -45°$. Additionally, the positions for 18 of the sources are south of $\delta = -60°$. The distribution of the position formal uncertainties is shown in Figure 2. The estimated positions have average formal uncertainties of 3.1 mas in $\alpha \cos\delta$ and 2.0 mas in δ. The formal uncertainties of the positions were *not inflated*, as was done for the ICRF and its extensions; that is, for the ICRF and its extensions it was assumed that for well-observed sources a more realistic estimate of their position errors could be made by inflating the formal errors by a factor of 1.5 followed by a root-sum-square increase of 0.25 mas (Ma et al. 1998; Fey et al. 2004a).

Note that since the three sources PKS 1143−696, 1156−663, and 1420−679 were also observed on the long (9595 km) baseline between South Africa and Australia, the positions of these sources are more precise than the positions of the remaining sources, which were observed on only the shorter (1089 km) intra-Australia baseline between Parkes and Hobart.

To facilitate the use of the 25 sources reported here as phase-reference calibrators, we list their correlated flux density from the 2004 May 12 observing session in Table 2. These values were obtained by comparing the observed signal-to-noise ratio (S/N) for each source derived from the correlation and fringe-finding process to the expected S/N, which was based on the scheduled on-source integration time and assumed a priori values of correlated flux density, receiver bandwidth, system temperature, and antenna sensitivity. The flux density scale was referenced to values of 0.8 Jy at 2.3 GHz and 1.9 Jy at 8.4 GHz for the ICRF source PKS 0405−385, which was observed as a position calibrator (see § 2). Correlated flux density values for PKS 0405−385 were obtained from the International VLBI Service[2] and were estimated from observations

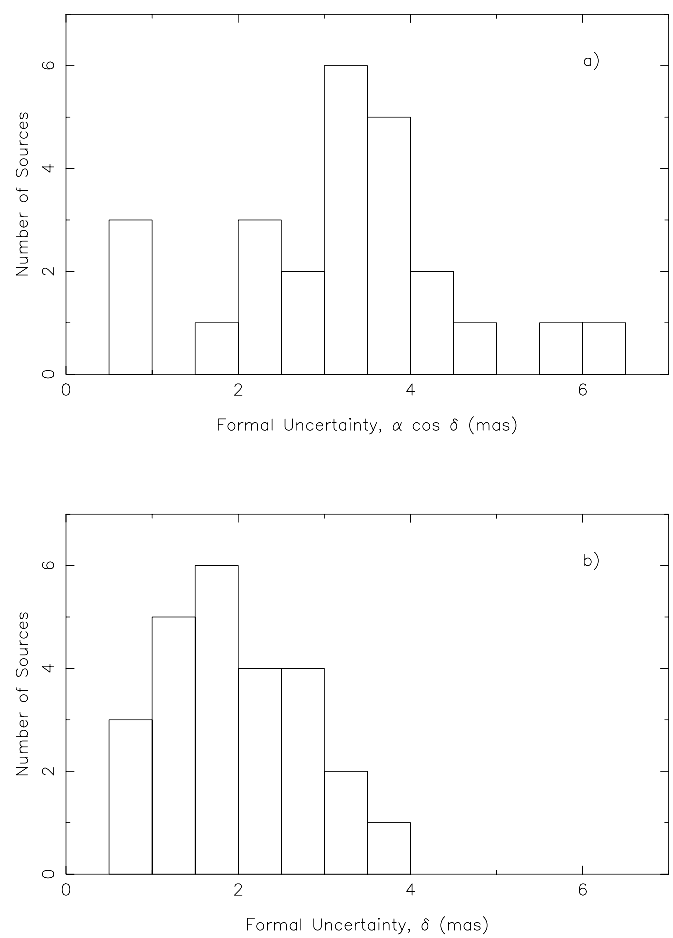

Fig. 2.—Distribution of position formal uncertainty in (*a*) $\alpha \cos\delta$ and (*b*) δ.

[2] See http://ivscc.gsfc.nasa.gov.

TABLE 2
CORRELATED FLUX DENSITY

Source	$S_{2.3\ \mathrm{GHz}}$[a] (Jy)	$S_{8.4\ \mathrm{GHz}}$[a] (Jy)
0037−593	0.4	0.2
0214−522	0.3	0.2
0542−735	0.2	0.3
0628−627	0.3	0.4
0744−691	0.2	0.3
0903−573	0.2	0.4
1005−739	0.1	0.2
1049−650	0.1	0.2
1133−739	0.1	0.2
1143−696	0.2	0.5
1156−663	0.2	0.3
1245−454	0.7	1.3
1303−827	0.1	0.2
1343−601	0.7	1.8
1417−782	0.1	0.3
1420−679	0.5	1.2
1448−648	0.3	0.3
1508−656	0.1	0.1
1611−710	0.3	0.4
1637−771	0.1	0.3
1725−795	0.2	0.6
2117−642	0.4	0.1
2215−508	0.5	0.2
2254−367	0.3	0.2
2311−477	0.3	0.2

[a] Values are correlated flux density measured on the Hobart-Parkes baseline on 2004 May 12.

TABLE 3
OPTICAL IDENTIFICATION OF SOURCES

Source	ID[a]	Magnitude	Redshift	Reference
0037−593	...	...	...	1
0214−522	G	23.0	...	2
0542−735	Q	20.1	...	3
0628−627	...	...	...	4
0744−691	Q	21.5	...	4
0903−573	Q	19	0.695	5
1005−739	Q	20.1	...	4
1049−650	Q	18.5	...	4
1133−739	...	21.6	...	4
1143−696	Q	17.7	...	4
1156−663	...	...	...	1
1245−454	...	...	...	...
1303−827	...	...	...	1
1343−601	G	10.75	0.013	6
1417−782	...	...	...	1
1420−679	Q	22.2	...	4
1448−648	G	22.0	...	4
1508−656	Q	22.0	...	4
1611−710	Q	20.7	...	4
1637−771	G	15.5	0.043	7
1725−795	Q	19.7	...	4
2117−642	...	...	...	1
2215−508	Q	17.4	1.356	8
2254−367	G	10.97	0.0056	9
2311−477[b]	...	...	...	3

[a] G = galaxy; Q = quasar.
[b] No optical object detected above the plate limit.
REFERENCES.—(1) NASA/IPAC Extragalactic Database (NED); no other reference; (2) Costa 2001; (3) Jauncey et al. 1989; (4) White et al. 1987; (5) Thompson et al. 1990; (6) West & Tarenghi 1989; (7) Simpson et al. 1993; (8) Jauncey et al. 1984; (9) Jackson et al. 2002.

taken on 2004 May 17 during an unrelated geodetic experiment. Optical information from the literature including identification, visual magnitude, and redshift, when known, for all 25 sources are listed in Table 3.

5. SUMMARY

We use new Mark III astrometric VLBI observations to estimate the radio positions of 25 southern hemisphere extragalactic sources. These results are part of an ongoing program intended to increase the number of phase-reference sources with accurate positions in the southern hemisphere for use in astrophysical observations. All sources have position estimates with formal uncertainties less than 10 mas in both coordinates, and all but one are located south of $\delta = -45°$. The reported positions are in the frame of the ICRF and thus can also be used to increase the sky density of southern hemisphere ICRF sources, although with reduced accuracy.

We would like to thank the staffs of the participating observatories for the time and effort required to make these observations. Additionally, we would like to thank the staff of the Washington Correlator for their hard work and dedication. This research has made use of the NASA/IPAC Extragalactic Database, which is operated by the Jet Propulsion Laboratory, California Institute of Technology, under contract with the National Aeronautics and Space Administration.

REFERENCES

Arias, E. F., Charlot, P., Feissel, M., & Lestrade, J.-F. 1995, A&A, 303, 604
Cannon, W. H., et al. 1997, Vistas Astron., 41, 297
Caprette, D., Ma, C., & Ryan, J. W. 1990, Crustal Dynamics Project Data Analysis, 1990 (NASA Tech. Memo. 100765) (Greenbelt: GSFC)
Clark, T. A., Corey, B. E., Davis, J. L., Herring, T. A., & Elgered, G. 1985, IEEE Trans. Geosci. Remote Sens., GE-23, 438
Costa, E. 2001, A&A, 367, 719
Fey, A. L., et al. 2004a, AJ, 127, 3587
———. 2004b, AJ, 127, 1791
Jackson, C. A., Wall, J. V., Shaver, P. A., Kellermann, K. I., Hook, I. M., & Hawkins, M. R. S. 2002, A&A, 386, 97
Jauncey, D. L., Batty, M. J., Wright, A. E., Peterson, B. A., & Savage, A. 1984, ApJ, 286, 498
Jauncey, D. L., Savage, A., Morabito, D. D., Preston, R. A., Nicolson, G. D., & Tzioumis, A. K. 1989, AJ, 98, 54
Johnston, K. J., et al. 1995, AJ, 110, 880
Kingham, K. A. 2003, in International VLBI Service for Geodesy and Astrometry 2002 Annual Report, ed. N. R. Vandenberg & K. D. Baver (NASA Tech. Pap. 211619) (Greenbelt: GSFC)
Lovell, J. E. J. 1997, Ph.D. thesis, Univ. Tasmania
Ma, C., et al. 1998, AJ, 116, 516
———. 1986, AJ, 92, 1020
Ma, C., Sauber, J. M., Bell, L. J., Clark, T. A., Gordon, D., Himwich, W. E., & Ryan, J. W. 1990, J. Geophys. Res., 95, 21991
McCarthy, D. D., ed. 1996, IERS Standards (1996) (IERS Tech. Note 21) (Paris: Obs. Paris)
Niell, A. E. 1996, J. Geophys. Res., 101, 3227
Ojha, R., et al. 2004, AJ, 127, 3609
Reynolds, J. E., Jauncey, D. L., Russell, J. L., King, E. A., McCulloch, P. M., Fey, A. L., & Johnston, K. J. 1994, AJ, 108, 725
Rogers, A. E. E. 1970, Radio Sci., 5, 1239
Russell, J. L., et al. 1992, AJ, 103, 2090

Russell, J. L., et al. 1994, AJ, 107, 379
Ryan, J. W., Ma, C., & Caprette, D. S. 1993, NASA Space Geodesy Program: GSFC Data Analysis, 1992; Crustal Dynamics Project VLBI Geodetic Results, 1979–1991 (NASA Tech. Memo. 104572) (Greenbelt: GSFC)
Ryan, J. W., Ma, C., & Vandenberg, N. R. 1980, The Mark III VLBI Data Analysis System (GSFC Publ. X-945-80-25) (Greenbelt: GSFC)
Simpson, C., Clements, D. L., Rawlings, S., & Ward, M. 1993, MNRAS, 262, 889
Thompson, D. J., Djorgovski, S., & de Carvalho, R. 1990, PASP, 102, 1235
West, R. M., & Tarenghi, M. 1989, A&A, 223, 61
White, G. L., Batty, M. J., Bunton, J. D., Brown, D. R., & Corben, J. B. 1987, MNRAS, 227, 705